INTERNATIONAL SOCIETY FOR SOIL MECHANICS AND GEOTECHNICAL ENGINEERING

SIMSG | ISSMGE

Comparison of Methodologies for Determining Soil Critical Shear Stress from Erosion Data

Haoyin Shan,[1] James Pagenkopf,[2] Otto Wiblishauser,[3] Chao Huang,[4] and Kornel Kerenyi[5]

[1]Genex Systems, Turner-Fairbank Highway Research Center (TFHRC) J. Sterling Jones Hydraulics Research Laboratory, 6300 Georgetown Pike, McLean, VA, 22101, USA; e-mail: haoyin.shan.ctr@dot.gov Corresponding author.
[2]Federal Highway Administration (FHWA), TFHRC J. Sterling Jones Hydraulics Research Laboratory, 6300 Georgetown Pike, McLean, VA, 22101, USA; e-mail: james.pagenkopf@dot.gov
[3]Genex Systems, TFHRC J. Sterling Jones Hydraulics Research Laboratory, 6300 Georgetown Pike, McLean, VA, 22101, USA; e-mail: o.wiblishauser.ctr@dot.gov
[4]Genex Systems, TFHRC J. Sterling Jones Hydraulics Research Laboratory, 6300 Georgetown Pike, McLean, VA, 22101, USA; e-mail: c.huang.ctr@dot.gov
[5]FHWA, TFHRC J. Sterling Jones Hydraulics Research Laboratory, 6300 Georgetown Pike, McLean, VA, 22101, USA; e-mail: kornel.kerenyi@dot.gov

ABSTRACT

Determining the erosion resistance, i.e., critical shear stress, of fine-grained soils through erosion testing is an essential aspect of the Federal Highway Administration's (FHWA) NextScour research initiative. FHWA has developed three erosion testing devices that can erode Shelby tube soil samples in the laboratory or the field. By eroding samples at various flow rates, the resulting erosion data can be used to compute the critical shear stress of the clay samples. Multiple methodologies were considered to calculate the critical shear stress value. A nonlinear power function was first adopted to calculate a deterministic value of the critical shear stress using a least squares method. However, typical erosion datasets from nonhomogeneous field soil testing contain scattered data points, making a probabilistic analysis of the erosion resistance more appropriate. The erosion data curves were reprocessed using shorter, overlapping time intervals to increase the number of data points for statistical analysis. The researchers compared the bin method and the bootstrapping technique to obtain mean, standard deviation, and coefficient of variation values for each dataset. These statistical values were then used to determine the distribution of the critical shear stress. When the distribution of critical shear stress was combined with hydraulic parameters, such as the variation of flood occurrence, channel roughness estimates, and hydrological and hydraulic modeling, i.e., the hydraulic load aspect of NextScour research initiative, a probabilistic scour analysis was achieved. A bridge replacement project in Bay City, Michigan, compares critical shear stresses derived using these methodologies and introduces the application of the distribution of the critical shear stress in the probabilistic scour analysis.

INTRODUCTION

Accurately predicting scour depths at bridge foundations, including piers and abutments, is an ongoing challenge for the bridge designer. Current design equations published in FHWA's *Hydraulic Engineering Circular No. 18* (HEC-18) estimate scour based on simplified hydraulic loads expressed in terms such as predicted flow depth, velocity, and discharge from a hydraulic analysis for a given flood event (Arneson et al. 2012). Soil resistance is often expressed solely as the median grain size (D_{50}) of the stream bed material, which is an acceptable practice for noncohesive soils, such as sands. However, for fine-grained cohesive soils, such as clays, the D_{50} value produces overly conservative estimates.

Determining the erosion resistance, i.e., critical shear stress, of fine-grained soils through erosion testing is an essential aspect of the FHWA's NextScour research initiative (Shan et al. 2021a; FHWA 2023). As part of NextScour, FHWA has also developed decay functions in which hydraulic loads can be compared directly against the critical shear stress values of subsurface soils to more accurately estimate scour depths. This paper discusses how the critical shear stress calculation moved beyond a simple deterministic calculation to include a probabilistic analysis of erosion data for producing a distribution of critical shear stress. Results from a case study of erosion testing for the Lafayette Avenue Bridge for the Michigan Department of Transportation (MDOT) demonstrate the methodologies (FHWA 2023).

SUMMARY OF FHWA EROSION DEVICES

Over the past decade, FHWA's Hydraulics Research Laboratory at TFHRC has developed three erosion testing devices for measuring the erodibility of cohesive soil samples. One device, designed for a laboratory setting, is similar in principle to the Erosion Function Apparatus (EFA) erosion device (Briaud et al. 2011). The other two devices function within a Shelby tube for erosion testing in the field. All three FHWA devices work by applying a range of flow rates to a cylindrical soil surface and measuring the corresponding erosion rates. This section provides a summary of the various devices and an overview of some advantages and disadvantages of testing with each device, all of which are shown in Figure 1.

The Ex-situ Scour Testing Device (ESTD) is an automated erosion device with a 120-mm wide by 19-mm high by 1-m long rectangular acrylic test channel (Shan et al. 2011). An underwater laser scanner mounted on an industrial robotic arm scans the soil surface every 20 s, sending a quasi-instantaneous signal to the control program. The control program averages the scan data and compares them to a reference point on the surface of the test channel. If the average value is less than this reference point, a command is sent to the piston to extrude the sample to maintain a surface flush with the channel bed. The erosion rate is calculated from the sample extrusion rate. After erosion tests are complete, a separate series of tests using the direct shear sensor are conducted to convert flow rates into shear stress values (Shan et al. 2021a). The ESTD is shown in Figure 1A. The benefits of testing with the ESTD include a horizontal flow on the sample that mimics open-channel flow and the ability to directly capture shear stress on the soil surface. The downside of the device is that samples need to be transported to the laboratory, which increases the risk of disturbing the specimen.

All photos source: FHWA.

| *A. Ex-situ (ESTD).* | *B. In-situ (ISTD).* | *C. Portable (PSTD).* |

Figure 1. FHWA's three scour testing devices.

The In-situ Scour Testing Device (ISTD) is a field erosion device that can erode subsurface soils at depths up to 18 m at a bridge site (Shan et al. 2021b). The device comprises an innovative erosion head that operates within a Shelby tube. A conventional drill rig augers down to the desired testing depth. Next, a pump circulates water through a system of casing, hoses, and piping to the erosion head, where the water is redirected into a high-speed radial flow against the exposed soil surface. As the soil erodes, distance sensors in the erosion head continuously monitor the erosion and control an algorithm to maintain a constant gap between the erosion head and the soil surface. The speed at which the erosion head descends represents the erosion rate. Flow rates are converted to shear stress using calibration tests between the ESTD and ISTD. Figure 1B shows the ISTD at a bridge site. The main benefit of the ISTD is that soil is tested in situ at the bridge site, with minimum disturbances in sampling. ISTD downsides include a longer assembly time and the need for careful coordination between the drillers and the ISTD operators. Additionally, the tests are conducted underground and cannot be easily monitored.

A simplified version of the ISTD, the Portable Scour Testing Device (PSTD), addresses the ISTD's inefficiencies (Shan et al. 2021b). Instead of conducting the erosion test in the borehole at the desired soil testing depth, the sample is recovered by the drill crew and tested at ground level. Although the erosion test is no longer conducted in situ, the test is still conducted onsite, eliminating the need to transport the soil sample back to the laboratory. The Shelby tube mounts into a subframe attached to the water tank. The erosion head is then inserted into the Shelby tube. From this point, testing is identical to the ISTD method. The most significant benefit of PSTD is that erosion testing is decoupled from the geotechnical drilling operation, which increases the speed and efficiency of testing. Drillers can quickly recover all the necessary samples, and then the drill rig is free for conducting other geotechnical explorations at the site. Shelby tubes can be visually inspected for damage before testing, eliminating the risk of attempting an erosion test underground in a damaged tube. Finally, since the erosion test is conducted at ground level, the power requirements of the pump are reduced, and a smaller portable pump can be used. Figure 1C shows the PSTD at a field demonstration site.

DATA COLLECTION AND ANALYSIS

Despite the physical differences between FHWA's laboratory and field erosion testing devices,

the devices collect similar data, which, after preprocessing, can be analyzed using the same basic scripts. Both devices produce continuous position data time series which are used to calculate erosion rates. The ESTD device collects position data from the piston that extrudes the samples into the channel flow. The ISTD and PSTD field devices measure the position of the erosion head as the linear drive lowers it into the Shelby tube to maintain a constant gap with the eroding soil surface. All devices measure flow rate in liters per second. The flows are not directly comparable, but they are proportional between the ESTD and ISTD/PSTD. The ESTD collects laser scan surface data, which tracks the shape of the surface as it erodes. The erosion head of the ISTD and PSTD has four linear variable differential transformer (LVDT) sensors that also track the surface shape. With only four LVDT sensors, the resulting surface data are much cruder than the data from the laser scan but still provide valuable information about how the soil surface erodes.

A typical erosion test for all devices records continuously for multiple flow rates. The ESTD is programmed to start at 2 L/s, and increases by 1 L/s every 10 min until it reaches a maximum of 13 L/s. The range of flow rates for a specific soil will vary based on the individual soil properties and how quickly the soil erodes. For the field devices, the pump is operated manually using a combination of the pump's throttle and a gate valve to regulate the flow rate. Flow rates using the portable pump and valve had a range similar to the ESTD, from around 2 L/s to a maximum of 13 L/s. However, since field testing was conducted manually, data collection did not follow the same rigorous script. Flow rates were often maintained for longer periods of time, usually 15–30 min, and increases to the next flow rate varied between 1 and 2 L/s. These parameters were often decided during testing by how quickly the soil eroded in the tube.

To extract erosion rates, position data are plotted against time. The flow data often are plotted on the same graph using a secondary axis, which helps identify the beginning and end points of each flow rate. Other data can be considered as well, including sensor or scan data to estimate the gap distance, which can help determine if the dataset is reasonable. Once the beginning and end points are marked, the simplest way to calculate the erosion rate is to run a best fit line through the dataset. Figure 2 shows an ESTD dataset of a soil sample from Michigan. The left vertical axis is the relative depth, and the right axis is the flow rate. Best fit lines are shown over the position data. The slopes of the lines are the erosion rates, while the corresponding flow rates are averaged across the same range. As mentioned previously, ISTD and PSTD position and flow rate plots look similar to Figure 2, although the flow rates typically do not advance in consistent increments.

For the ESTD tests, flow rates are converted into shear stresses using a separate series of tests measuring shear stresses on soil samples using the direct shear sensor. FHWA researchers also established a general relationship to convert ESTD flow into shear using field soil samples, engineered soils samples, and non-erodible discs in the shear sensor. This relationship is similar to the pipe-flow shear stress formula using a friction factor obtained from the Moody diagram (Moody 1944). For ISTD data, a separate equation was used to convert ISTD flow rates to an equivalent shear stress value. That equation was developed based on a comparison study between the ISTD and ESTD devices eroding engineered soil samples.
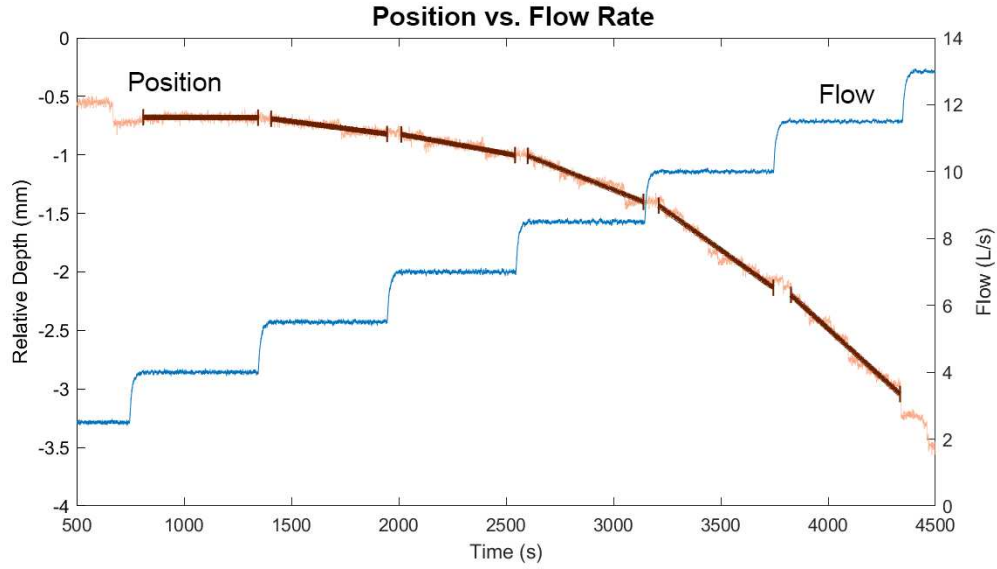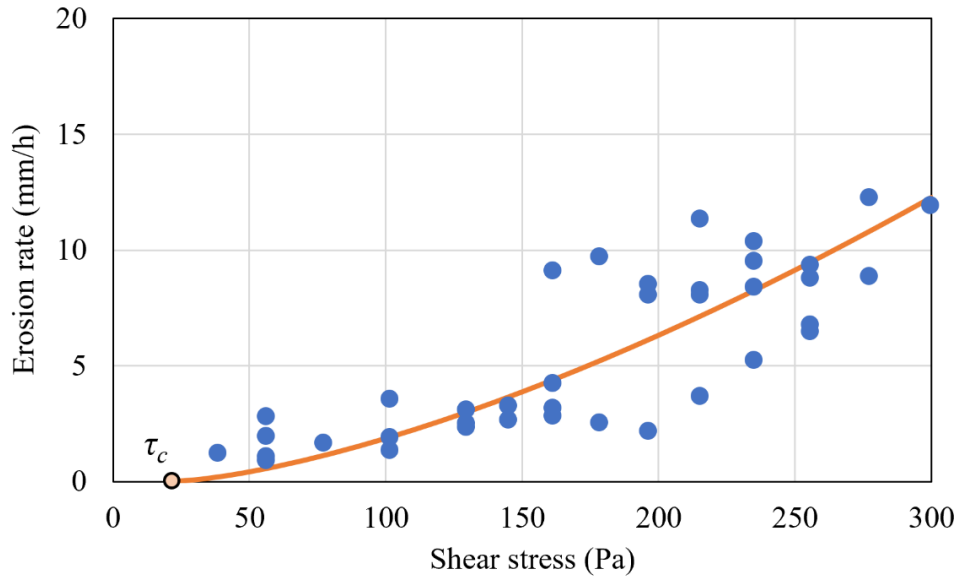
Source: FHWA.

Figure 2. Typical raw erosion data with best fit lines for six different flow rates.

Deterministic Power Curve

Erosion rate data points are plotted against shear stress, as shown in Figure 3. The relationship generally follows a power function. Critical shear stress, τ_c, is defined as the bed shear stress where incipient motion begins and can be incorporated into the power function as shown in Eq. 1, where $\dot{e}$ is erosion rate, τ is shear stress, and a and b are equation constants. Eq. 1 can be determined by fitting the three parameters a, b, and τ_c, using a nonlinear least squares approach for each set of test data.

$$\dot{e} = a(\tau - \tau_c)^b \tag{1}$$

Source: FHWA.

Figure 3. ESTD erosion data with power curve fit to determine critical shear stress.

5

While this approach generally worked for engineered soils with homogeneous properties, applying it to field soil datasets was difficult. Repeatability was an issue with the nonlinear solver. Modifying the dataset slightly or adjusting the initial conditions would produce significant changes in the final results. Often, the fitting wanted τ_c to converge to zero, which was not an acceptable outcome. If limits were entered into the solver to constrain the output, the final results would occasionally equal one of the limit values. Unfortunately, Eq. 1 was difficult to apply consistently in practice. This was apparent with field data from the Lafayette Avenue Bridge project. When data points from a single Shelby tube were plotted and fitted with Eq. 1 (similar to the example in Figure 3), the τ_c converged to zero as there were too many datapoints to optimize the least squares fit.

PROBABILISTIC DATA ANALYSIS METHODOLOGY

Alternative methods to calculate critical shear stress using probabilistic analyses were explored. One of the biggest advantages of data collection using the ESTD, ISTD, or PSTD is that all collect continuous time-series erosion data. Ideally, erosion occurs in a smooth, consistent, and predictable manner, but that often was not the reality, especially for field soils. Frequently, the position data contained sudden drops reflecting clumps of soil eroding in the flow. A single best fit line cannot accurately capture a short, sudden erosion of material that occurs in the middle of the test run. However, splitting the data series into smaller time windows can capture these instances and their frequency.

Different window sizes varying from 30 to 240 s were considered along with a variety of time shifts (or overlaps). Shorter windows and greater overlap can produce more data points, but window sizes shorter than 60 s were potentially prohibited by the ESTD laser scan cycle of 20 s.

Bin Method
The first probabilistic method considered was the bin method, which divided the data into a series of horizontal bins. Horizontal bins allowed sampling across multiple clusters, where data were clustered based on flow rates. A mean value, standard deviation, and coefficient of variation (COV) can be calculated from the subset of data points in each bin. By looking at the trend in the mean values, one could then extrapolate to find the critical shear stress of the soil.

The number of horizontal bins used in the analysis was calculated as the log-base 2 of the total number of data points. Each bin contained an equal number of data points. For each bin, the mean, standard deviation, and COV were calculated for both erosion rate and shear stress values. Figure 4 shows thousands of data points ranging between 2 and 20 mm/h, split into 11 bins from ESTD erosion testing for the Lafayette Avenue Bridge project (FHWA 2023). Data below 2 mm/h were excluded from this exercise because they skewered the fit.
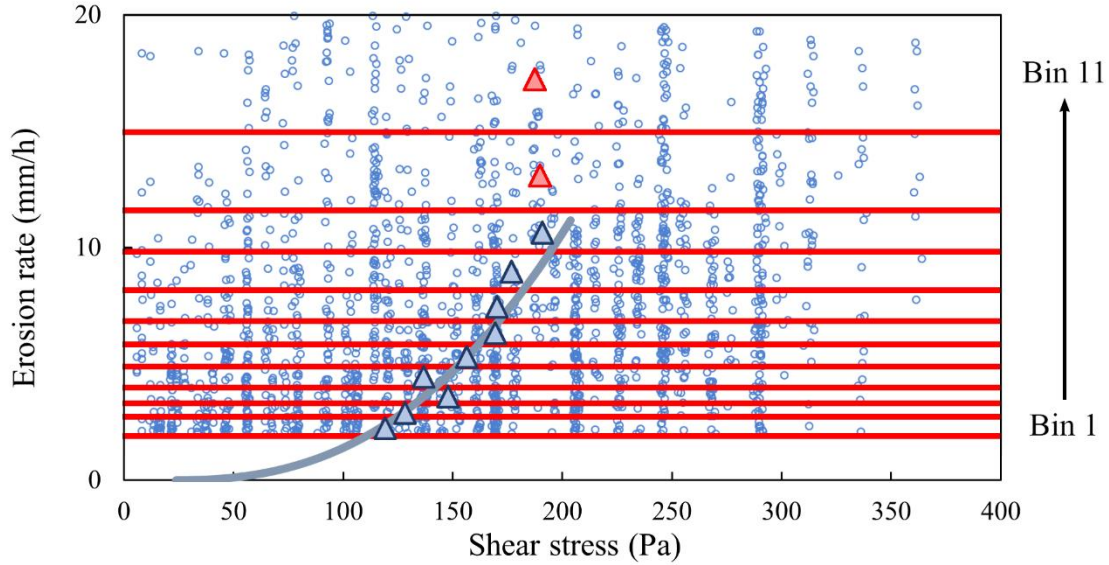
Figure 4. Power curve fit through bin mean values.

For the Lafayette Avenue Bridge project, all data points collected from nine Shelby tube samples were combined. If subsurface soil layers vary at a test site, each soil type can be analyzed separately. Five different time window durations were evaluated, as well as two different time shifts. Each analysis produced a set of mean values, and then Eq. 1 was applied to the final set of mean data points to extract the critical shear stresses. Because the least squares fit was applied to the mean bin values, small variations in the data points did not affect the final critical shear stress result. However, the bin method did not resolve the other prior issues related to using a nonlinear solver. Whether the variability calculated with this method reflected soil properties or the data window properties was also unclear.

Bootstrapping Method
The second probabilistic method considered was the bootstrapping method (Stine 1989). In this method, the data are plotted on a log-log plot, and from the cloud of data points, a subset is selected at random. From this subset, a log-log best fit line is calculated. This process is repeated N times, from 5,000 to 50,000. A higher N value will produce a smoother distribution. A sensitivity analysis found that a minimum of 5,000 iterations produced similar results for each attempt. For this method, a nonzero erosion rate was selected to determine the critical shear stress value, in this case 0.1 mm/h, which matched the definition used by Briaud et al. (2011). The intersection of the best fit lines at the selected erosion rate results in a distribution of critical shear stress values, from which a COV can also be calculated.

The first step of the bootstrapping method was to apply a power function to describe the erosion function of the cohesive soil tested, as follows:

$$\dot{e} = k_a \tau^{k_b} \tag{2}$$

where k_a and k_b are equation constants similar to a and b. By taking the logarithm of both sides, Eq. 2 converts to a linear relationship (as shown in Eq. 3), and a linear best fit was applied to the

data to obtain constants k_a and k_b. After fitting both constants, the critical shear stress was computed when the erosion rate equaled 0.1 mm/h, as follows:

$$\log(\dot{e}) = \log(k_a) + k_b \times \log(\tau) \tag{3}$$

The Lafayette Avenue Bridge project erosion data were divided into 4-min time windows, with 2-min overlaps between adjacent windows. For very low flows, where erosion may not be detectable by the ESTD's laser, a lower boundary for erosion was set at 0.016 mm/h, which was based on the resolution of the laser scanner. In total, 1,127 erosion data points were plotted, as shown in Figure 5. The solid line represents the linear fit function for the complete dataset. With the corresponding fitted constants k_a of 0.00033 and k_b of 1.89, the critical shear stress was calculated to be 20.5 Pa.
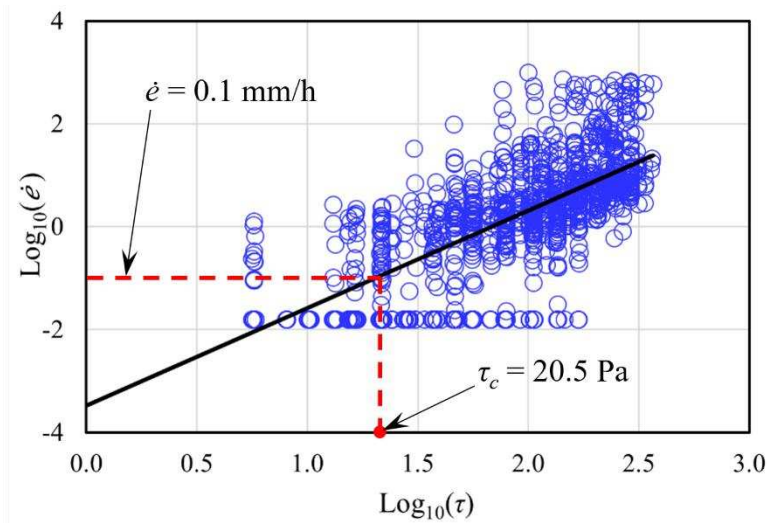
Source: FHWA.

**Figure 5. Logarithmic best fit of erosion data (FHWA 2023).**

The second step of the bootstrapping method was to randomly select a subset of data points from the entire set and apply the logarithmic best fit equation. A script randomly selected 40 out of the 1,127 data points and applied the best fit function to calculate a corresponding critical shear stress. The subset value of 40 was selected as a reasonable number of data points to collect from two 305-mm Shelby tube samples. This process was repeated 50,000 times to get a distribution of linear best fits (Figure 6). The two dashed lines represent the 95-percent confidence limits on the linear fit of the mean critical shear stress, and the solid line is the mean linear fit of the 50,000 iterations. The distribution of critical shear stresses was found by intersecting the linear fits with the erosion rate of $\dot{e} = 0.1$ mm/h. Figure 7 plots a histogram of all 50,000 critical shear stresses. The mean value of the critical shear stresses was 20.5 Pa, which matched the value calculated previously for the entire 1,127-point dataset. The standard deviation was 6.56 Pa, and the COV was 0.32. Both mean and COV were used as the critical shear stress distribution parameters. Since the erosion rates follow a lognormal distribution, the distribution of the critical shear stress was also assumed lognormal.
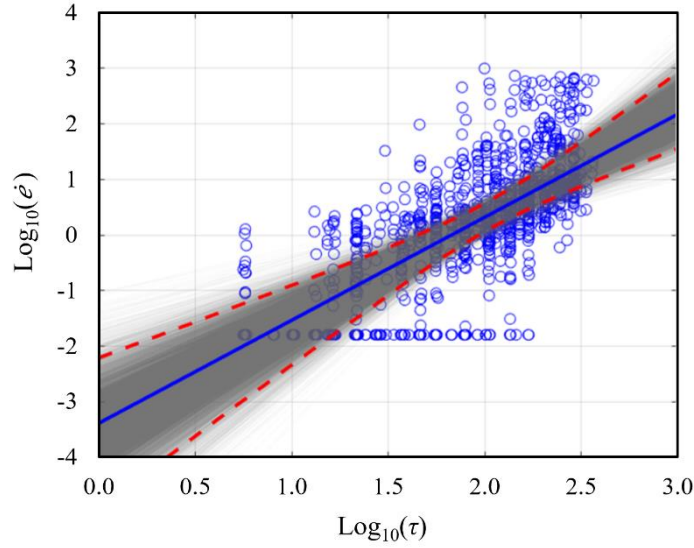
Note: Dashed lines represent the 95-percent confidence interval on the mean linear fit.

Figure 6. Bootstrapping technique showing 50,000 linear fittings (FHWA 2023).
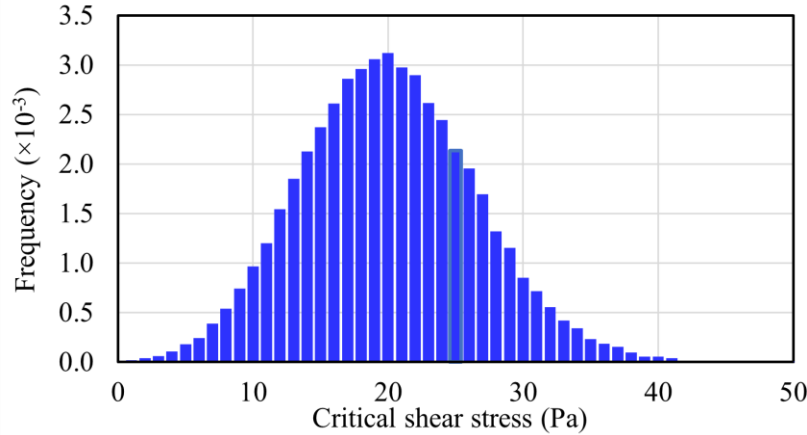
Figure 7. Histogram of the 50,000 critical shear stresses (FHWA 2023).

Of the two probabilistic analysis methods studied by FHWA, the bootstrapping method was preferred because it generated more reliable and reproducible distributions of the critical shear stress from the erosion datasets.

CONCLUSIONS

Erosion data collected from FHWA's scour testing devices were used to determine the critical shear stresses of cohesive soils. These devices, including the ESTD, ISTD, and PSTD, produce continuous position data that can be divided into smaller windows, increasing the amount of data points and more accurately capturing fluctuating erosion conditions. This study comprised two probabilistic analysis methods, the bin method and the bootstrapping technique, to produce a

distribution of critical shear stress. The bootstrapping method was preferred because it provided consistent mean, standard deviation, and COV of the critical shear stress. These data provide the ability to conduct a probabilistic scour analysis.

Potential future research may include variations of the bootstrapping method, including applying a time-series bootstrap to randomize the size and location of the data windows. Smoothing filters may also be tested to reduce the influence of the laser scan and piston push step cycle. As more soils are tested with advanced methodologies, FHWA researchers believe that correlations can be established between soil indexing properties and their critical shear stress values.

REFERENCES

Arneson, L., Zevenbergen L., Lagasse, P., and Clopper, P. (2012) *Hydraulic Engineering Circular No. 18, Evaluating Scour at Bridges, Fifth Edition.* Report No. FHWA-HIF-12-003. Federal Highway Administration, Washington, DC.

Briaud, J. L., Chen, H. C., Chang, K. A., Oh, S. J., Chen, S., Wang, J., Li, Y., Kwak, K., Nartjaho, P., Gudaralli, R., Wei, W., Pergu, S., Cao, Y. W., and Ting, F. (2011) *The SRICOS—EFA Method Summary Report.* Texas A&M University, College Station, TX.

Federal Highway Administration. (2023) *NextScour Case Study: The Lafayette Avenue Bridge over the Saginaw River in Bay City, Michigan.* Report No. FHWA-HRT-23-104, Federal Highway Administration, Washington, DC.

Moody, L. F. (1944) "Friction Factors for Pipe Flow." *Transactions of the American Society Mechanical Engineers*, 66, no. 8: 671–684.

Shan, H., A. Wagner, K. Kerenyi, J. Guo, and Z. Xie. 2011. "An Ex-Situ Scour Testing Device for Erosion Research of Cohesive Soils." *Proceedings of the 2011 Engineering Mechanics Institute Conference.* Boston, MA: American Society of Civil Engineers. 1020–1027.

Shan, H., Pagenkopf, J., Kerenyi, K., and Huang, C. (2021a) "NextScour for Improving Bridge Scour Design in the United States." *Proc. of the Institution of Civil Engineers–Forensic Engineering,* 173(4), 121–129, https://doi.org/10.1680/jfoen.20.00017, last accessed October 5, 2022.

Shan, H., Pastrich, D., Pagenkopf, J., Wiblishauser, O., Uhrig, M., Nagy, N., Zuelow, C., Ghelardi, V., Alzamora, D., Mohamed, K., Kerenyi, K., and Huang, C. (2021b) "In-situ Scour Testing Device Demonstrations at 18 State Departments of Transportation." *Proc. of the 10th International Conference on Scour and Erosion*, American Society of Civil Engineers, Arlington, VA.

Stine, R. (1989) "An Introduction to Bootstrap Methods: Examples and Ideas." *Sociological Methods and Research*, 18(2–3), 243–291.